Symbolic Regression for Data-Driven Dynamic Model Refinement in Power Systems

Andrija T. Sarić, *Member, IEEE*, Aleksandar A. Sarić, *Student Member, IEEE*, Mark K. Transtrum, and Aleksandar M. Stanković, *Fellow, IEEE*

Abstract—This paper describes a data-driven symbolic regression identification method tailored to power systems and demonstrated on different synchronous generator (SG) models. In this work, we extend the sparse identification of nonlinear dynamics (SINDy) modeling procedure to include the effects of exogenous signals (measurements), nonlinear trigonometric terms in the library of elements, equality, and boundary constraints of expected solution. We show that the resulting framework requires fairly little in terms of data, and is computationally efficient and robust to noise, making it a viable candidate for online identification in response to rapid system changes. The SINDy-based model identification is integrated with the manifold boundary approximation method (MBAM) for the reduction of the differential-algebraic equations (DAE)-based SG dynamic models (decrease in the number of states and parameters). The proposed procedure is illustrated on an SG example in a real-world 441-bus and 67-machine benchmark.

Index Terms—Power system, dynamic model, system identification, nonlinear dynamics, symbolic regression.

I. INTRODUCTION

DENTIFICATION of a dynamical system from data (recorded measurements) has been an important problem in mathematical physics, with a long history in power systems [1]–[5]. Many techniques in system identification, including dynamic mode decomposition (DMD) (for example, [6]), equation-free modeling (for example, [7]), cluster reduced-order models based on the probabilistic transition between various system behaviors (for example, [8]) and many other algorithms are designed to handle high-dimensional data. DMD in particular has strong connections to nonlinear dynamics through Koopman operator theory (for example, [9]).

Manuscript received April 29, 2020; revised August 12, 2020; accepted October 17, 2020. Date of publication October 22, 2020; date of current version April 19, 2021. This work was supported in part by NSF under Grant ECCS-1710944, in part by CURENT Engineering Research Center of the National Science Foundation and the Department of Energy under NSF Award Number EEC-1041877, and in part by ONR under Grant N00014-16-1-3028. Paper no. TPWRS-00709-2020. (Corresponding author: Aleksandar M. Stankovic.)

Andrija T. Sarić is with the Department for Power, Electronic and Communication Engineering of the Faculty of Technical Sciences, University of Novi Sad, Novi Sad 21000, Serbia (e-mail: asaric@uns.ac.rs).

Aleksandar A. Sarić and Aleksandar M. Stanković are with the Department of Electrical Engineering and Computer Science of Tufts University, Medford, MA 02155 USA (e-mail: aleksandar.saric@tufts.edu; astankov@ece.tufts.edu).

Mark K. Transtrum is with the Department of Physics and Astronomy, Brigham Young University, Provo, UT 84602 USA (e-mail: mktranstrum@byu.edu).

Color versions of one or more of the figures in this article are available online at https://ieeexplore.ieee.org.

Digital Object Identifier 10.1109/TPWRS.2020.3033261

Once parameters of a dynamic model have been optimized to match recorded responses (or data generated from a more detailed model), there typically exists a difference (or error) between the model prediction and the target waveform. A question of great interest then is if there exists a structure in the error that can be utilized to possibly improve the model while maintaining the practical identifiability that is critical for model utility. If the original model has established physical plausibility, it makes sense to try to append it, possibly with portions that capture additional features. These new facets are preferably also based on physics to maintain the model's overall interpretability and portability [10].

One promising idea for deriving and appending possibly nonlinear models is symbolic regression, and the sparse identification of nonlinear dynamics (SINDy) based solution method [11]–[13]. It operates in the space of mathematical expressions and attempts to find the best fit for data while balancing requirements for accuracy and simplicity (e.g., a small number of terms in an expression). The candidate mathematical expressions belong to families that are typically pre-selected and include standard types often found in physics-derived engineering models like constants, polynomials, trigonometric terms, etc. It is, of course, evident that the space of candidate models is very large regardless of the parametrization selected, and that any solutions found will likely be non-unique and possibly locally optimal.

Our starting point is the equation-based modeling framework [13]. The authors leverage the fact that most dynamical systems of engineering interest have relatively few nonlinear terms, each belonging to a known family (e.g., polynomials), to devise a data-driven algorithm for the SINDy. One key idea is to rely on sparsity-promoting techniques throughout the model development so that the result balances accuracy with the number of terms included. Control inputs were added to the algorithm in [14].

One problem that is well suited to this framework is the transient stability of large power systems, because it focuses on system-wide behavior, and de-emphasizes component-level accuracy. In transient stability, the dynamic behavior stems mostly from component dynamics, which is typically described by models that have a limited number of entries on the right-hand side. The size of the network matters, of course, but since dynamic components are connected in nodes, their behavior is altered by (algebraic) variables at the point of connection (such as voltages, angles, and active/reactive powers). Hence the overall model preserves sparsity. We intend to use past the physical

 $0885\text{-}8950 \ @\ 2020\ IEEE.\ Personal\ use\ is\ permitted,\ but\ republication/redistribution\ requires\ IEEE\ permission.$ See https://www.ieee.org/publications/rights/index.html for more information.

understanding of key phenomena to restrict and customize the set of building blocks that need to be included in the regression. This paper advances a Galerkin-type regression method [11] for identification of non-linear dynamics in SINDy with actuation (measurements) and physical equality and boundary constraints to identify system-wide aspects of dynamic components (in our case on an SG example). Motivated by the structure of the typical power system equations, the library of dynamical elements in SINDy is extended with mixed products of linear and trigonometric functions of states, algebraic variables, and external signals (measurements).

A large body of references on power system dynamics [1]–[4], including our preliminary work [5], [15], has concluded that many common models of power system transients have good physical justifications, but tend to be practically unidentifiable from commonly available measurements. We use MBAM to prescreen and modify dynamic models, making them practically identifiable before we attempt sparse identification via SINDy.

Main contributions (compared with our initial work reported in [15]) may be summarized as:

- Respecting the structure of the typical power system equations (on the analyzed SG's test example), the library of dynamical elements in SINDy is extended with typical mixed nonlinear (trigonometric) multiplications of measurement and state/algebraic variable functions (Section III-B).
- The SINDy algorithm with measurements, equality, and boundary constraints of the expected solution is proposed in Section III-C.
- Based on the conclusions of [15] that the SG's model identification is not a straightforward task, several optimization tools are investigated for the solution of the specified bound-constrained least-squares optimization model.
- Optimization of differences between measurements and calculated time responses for a single SG with a reduced vector of states, subjected to the differential and algebraic equations based constraints.
- Integrated DAE- and MBAM-based dynamic model reduction with SINDy-based model identification (Section V).
- Gray-box integration of physics-driven model (DAE-based for reduced dynamic model) and data-driven model (for differences between available measurements and calculated transient responses for reduced dynamic model).
- Application on a realistic example (441-bus real-world power system, compared with the IEEE 14-bus example in [15]).

The outline of the paper is as follows: Section II provides the problem formulation; Section III describes the SINDy algorithm with extended the library of dynamical elements, as well as with external measurements, equality, and boundary constraints; in Section IV the MBAM-based algorithm for dynamic model reduction is described; Section V integrates the SINDy and MBAM (parameter identification and dynamic model reduction, respectively); the proposed algorithm is applied to an SG example in Section VI; Section VII presents conclusions. The Appendix contains basic SG's equations and parameters adapted for SINDy-based model identification.

II. PROBLEM FORMULATION

The DAEs-based form of power system dynamic model used in transient stability is

$$\dot{\boldsymbol{x}} = \boldsymbol{f}(\boldsymbol{x}, \boldsymbol{z}, \boldsymbol{p}, t) \tag{1}$$

$$\mathbf{0} = \mathbf{g}(\mathbf{x}, \mathbf{z}, \mathbf{p}, t) \tag{2}$$

where x is the vector of (differential) state variables, z are the algebraic variables, p is the vector of parameters, and t is the (scalar) time variable.

System measurement vector is assumed to be of the form

$$y = h(x, z, p, t) \tag{3}$$

System identification is the standard approach to find the best parameters to minimize discrepancies between measured (y) and corresponding calculated (y^c) time responses

$$p = \underset{p}{\operatorname{argmin}} \|y - y^{c}\|_{2}^{2}$$
 (4)

subject to (1)–(3).

For analyzed SG test examples, details of differential (f), algebraic (g), and measurement equations (h) in (1)–(3), respectively, are given in Appendix A and in [5].

III. SPARSE IDENTIFICATION OF NONLINEAR DYNAMICS (SINDY) ALGORITHM

The SINDy algorithm identifies possibly fully nonlinear dynamical systems [in our case, functions f in (1) and g in (2)] from the available data set [in our case, functions h in (3)]. It is the counterpart of ideas on dictionary learning and dictionary-based regression that are widely used in compressed sensing literature [16], [17] and relies on the fact that in this application, we expect the right-hand side of (1) and (2) to be (very) sparse.

A. Basic SINDy Algorithm [11]–[14]

Formally, the dynamic model may be written in the following form

$$\dot{X} = \Theta(X)\Xi \tag{5}$$

where $\Theta(\boldsymbol{X})$ is a library of dynamical elements (see Section III-B for more details), Ξ is $(K \times N_x)$ -dimensional matrix, K is the total number of constant, linear, and non-linear functions, and N_x is the total number of state variables in \boldsymbol{X} .

We collect a time history of the total N_x state variables x(t) in (5), sampled at time series $t_1, \ldots, t_t, \ldots, t_{N_t}$, as $(N_t \times N_x)$ -dimensional matrix

$$X = \begin{bmatrix} x_1 & \cdots & x_n & \cdots & x_{N_x} \end{bmatrix}$$

$$= \begin{bmatrix} x_1(t_1) & \cdots & x_n(t_1) & \cdots & x_{N_x}(t_1) \\ \vdots & \ddots & \vdots & \ddots & \vdots \\ x_1(t_t) & \cdots & x_n(t_t) & \cdots & x_{N_x}(t_t) \\ \vdots & \ddots & \vdots & \ddots & \vdots \\ x_1(t_{N_t}) & \cdots & x_n(t_{N_t}) & \cdots & x_{N_x}(t_{N_t}) \end{bmatrix}$$

$$(6)$$

where N_t is the total number of time points.

Matrix Ξ in (5) is sparse for most dynamical systems (including power system dynamics). For identification of Ξ , the sparse symbolic regression may be applied.

Each of the N_x column equations in (5) is determined by the sparse K-dimensional vector of coefficients ξ_n , corresponding to the *n*-th column of \hat{X} (\hat{X}_n) and $\Xi(\xi_n)$ which can be found using a sparse separate regression algorithm [13], as

$$\boldsymbol{\xi}_n = \underset{\boldsymbol{\xi}_n}{\operatorname{argmin}} \|\boldsymbol{\Theta}(\boldsymbol{X})\boldsymbol{\xi}_n - \dot{\boldsymbol{X}}_n\|_2^2 + \lambda^2 \|\boldsymbol{\xi}_n\|_1$$

$$n = 1, 2, \dots, N_x$$
(7)

where $\boldsymbol{X}_n \equiv \boldsymbol{x}_n = x_n$ (t) represents n-th column (time response of n-th state variable) of X in (6).

$$\dot{x}_n(t_{t-2}) = \frac{-x_n(t_{t+2}) + 8x_n(t_{t+1}) - 8x_n(t_{t-1}) + x_n(t_{t-2})}{12\Delta t}$$

$$t \neq 1, 2, N_t - 1, N_t$$
 (8)

where $\Delta t = t_t - t_{t-1}$ is the sampling interval.

The penalty term $\|\cdot\|_1$ in (7) promotes sparsity in the vector $\boldsymbol{\xi}_n$. Note that the convex norm $\|\boldsymbol{\xi}_n\|_1$ in (7) replaces the nonconvex (pseudo)norm $\|\boldsymbol{\xi}_n\|_0$ (the number of non-zero entries of the vector $\boldsymbol{\xi}_n$). The parameter λ in (7) is selected to identify the optimal model that best balances low model complexity with accuracy. A coarse sweep of λ is performed to identify the rough order of magnitude, where terms are eliminated and where the error begins to increase [19].

B. The Library of Candidate Dynamics for Power System **Based Equations**

The selection of the library of candidate dynamics is a crucial choice in the SINDy-based algorithm(s).

Note that in a power system case several characteristic examples may appear (we are limited here only to the analyzed SG parameter identification example):

- mixed nonlinear (trigonometric) multiplications of measurements and state/algebraic variables, $y_i \sin(x_i - z_k)$ [for example, $\frac{(x_q-x_q')}{x_q'}V\sin(\delta-\theta)$ —see Appendix A];
 • mixed nonlinear (trigonometric) multiplications of states
- and state/algebraic variables, $x_i \sin(x_i z_k)$ [for example, $\frac{Ve'_q}{x'}\sin(\delta-\theta)$ —see Appendix A].

To simplify the presentation, in this section we assume that only state variables-based dynamics (1), $\Theta(X)$ in (7), will be identified. This assumption will be relaxed later in Section III-C with additional identification of algebraic variables and measurements, or $\Theta(X, Z, Y)$.

A library of K candidate constant, linear and non-linear functions $\Theta(X)$ of the columns of X in (6) may consist of polynomial and trigonometric terms, as well as their products, and symbolically may be written as

$$\Theta(X) = [\operatorname{Const} X X^{2} \sin(X) X \sin(X) \cdots] \quad (9)$$

where $\Theta(X)$ is $(N_t \times K)$ -dimensional matrix and any term in (9) introduces the appropriate number of column-vectors.

For example, two typical terms in (9) are as follows:

 \boldsymbol{X}^2

$$= \begin{bmatrix} x_1^2\left(t_1\right) & x_1\left(t_1\right)x_2\left(t_1\right) & \cdots & x_2^2\left(t_1\right) & \cdots & x_{N_x}^2\left(t_1\right) \\ \vdots & \vdots & \ddots & \vdots & \ddots & \vdots \\ x_1^2\left(t_t\right) & x_1\left(t_t\right)x_t\left(t_t\right) & \cdots & x_2^2\left(t_t\right) & \cdots & x_{N_x}^2\left(t_t\right) \\ \vdots & \vdots & \ddots & \vdots & \ddots & \vdots \\ x_1^2\left(t_{N_t}\right) & x_1\left(t_{N_t}\right)x_2\left(t_{N_t}\right) & \cdots & x_2^2\left(t_{N_t}\right) & \cdots & x_{N_x}^2\left(t_{N_t}\right) \end{bmatrix}$$

 $X \sin(X)$

The library of dynamical functions $[\Theta(X)]$ in (7) may be simply extended to support other nonlinearities (for example, saturation, exponential terms in dynamic load models, etc.).

A detailed mathematical proof of convergence of the SINDy algorithm may be found in [20].

For more details about the SINDy algorithm application and its convergence on the simplified SG's test example, please see [15, Section V]. These results show a clear discrepancy in some cases. We see several reasons for the inconsistency when using the basic SINDy formulation (from Section III-A), as used in [15]:

- 1) we determine the right-hand side through numerical differentiation (8), which, despite our effort to use numerically sound procedures, inevitably introduces errors;
- 2) the "true" system used in identification is a system of DAEs (1)–(3), while the basic SINDy algorithm assumes pure differential system; while many power systems are believed to be described by index-1 DAE (we do not check this condition);
- 3) ref. [20] uses the 0-(pseudo)norm do characterize the support of the solution, while we use the 1-norm (this is standard in practice);
- 4) the model we are considering is inherently stiff numerically, as the coefficient Ω_b in differential equation for δ (the derivative of the rotor angle transient response) is several times larger than the other coefficients, and there exists a weak functional coupling of the differential equation for δ with other differential equations [see (A1) in Appendix A].

Based on the above conclusions, in the next section we propose a modified formulation (11)–(13), which works much better on power system problems, but most likely has different convergence conditions.

C. The SINDy Algorithm With Constraints and Measurements

The SINDY algorithm from Section III. A may be generalized to include fully nonlinear dynamics in additional functions [g in (2) and h in (3)], algebraic variables (z), and actuation (measurements) (y), respectively, since this merely requires building a larger library $\Theta(X, Z, Y)$ of candidate functions, that additionally includes the ($N_t \times N_z$)-dimensional matrix of time-dependent N_z algebraic variables (Z) and the ($N_t \times N_y$)-dimensional matrix of time-dependent N_y measurements (Y), as in (5) and all mixed cases among X, Z, and Y (notice that a total number of columns in $\Theta(X, Z, Y)$ is typically $K > N_x + N_z + N_y$ due to include the mixed product of variables and measurements of state and algebraic variables)

$$\left[\dot{X} Z Y\right] = \Theta(X, Z, Y) \Xi_{x,z,y} \tag{10}$$

where $\Xi_{x,z,y} = [\Xi_x \; \Xi_z \; \Xi_y]$.

In this case, the optimization problem (7) with additional equality and boundary constraints may be rewritten as

$$\boldsymbol{\xi}_n = \operatorname*{argmin}_{\boldsymbol{\xi}_n} \|\boldsymbol{\Theta}(\boldsymbol{X}, \boldsymbol{Z}, \boldsymbol{Y})_n \boldsymbol{\xi}_n - \left[\dot{\boldsymbol{X}} \ \boldsymbol{Z} \ \boldsymbol{Y} \right]_n \|_2^2 + \lambda^2 \|\boldsymbol{\xi}_n\|_1$$

$$n = 1, 2, \cdots, (N_x + N_z + N_y)$$
 (11)

subject to:

$$g(X, Z, Y) = 0 (12)$$

$$\boldsymbol{\xi}_n^{\min} \le \boldsymbol{\xi}_n \le \boldsymbol{\xi}_n^{\max} \tag{13}$$

where in (12) we include the equality constraints from (2) and (3). Please note that formulation (11)–(13) differs from the original SINDy formulation (7), so its convergence conditions [20] are explored via numerical experiments later.

Lower and upper bounds in (13) are used to enforce that some entries of ξ_n in the predefined intervals around physically reasonable values [see (A3) and (A4) in Appendix B for details].

The optimization problem (11) and (12) may be transformed to the unconstrained problem using an augmented formulation, where the constraints are imposed via Lagrange multipliers (to simplify the formulation, the λ term is omitted), as

$$\boldsymbol{\xi} = \sum_{n=1}^{N_x + N_z + N_y} \left(\underset{\boldsymbol{\xi}_n, \boldsymbol{\varsigma}}{\operatorname{argmin}} \|\boldsymbol{\Theta}(\boldsymbol{X}, \boldsymbol{Z}, \boldsymbol{Y}) \boldsymbol{\xi}_n - \left[\dot{\boldsymbol{X}} \ \boldsymbol{Z} \ \boldsymbol{Y} \right]_n \|_2^2 \right) + \boldsymbol{\varsigma}^{\mathrm{T}} \boldsymbol{q}(\boldsymbol{X}, \boldsymbol{Z}, \boldsymbol{Y})$$
(14)

The optimal solution (ξ) is a solution to the Karush-Kuhn-Tucker (KKT) equations [11, eq. (2.10)].

Note that the measurement vector (y) may contain state variables (x), algebraic variables (z), and their nonlinear combinations (for example, measurement $P_g(t)$ in function h; for practical aspects, see Section VI-A).

IV. THE MANIFOLD BOUNDARY APPROXIMATION METHOD (MBAM) FOR DYNAMIC MODEL REDUCTION

The MBAM is a parameter reduction algorithm that uses information geometry methods, i.e., application of differential geometry to statistics [21]–[23]. The basic idea is that a parameterized model is interpreted as a manifold of potential

predictions. Distances on the manifold are induced by distinguishability of model parameters from data using information theory. If different parameter values lead to nearly identical predictions, they correspond to nearby points on the manifold and, conversely, parameter values that lead to very different predictions are distant on the manifold.

Many models have bounded manifold. Boundaries correspond to limiting cases of parameter values such as relevant time scales going to zero as in singular perturbation. Parameters are practically unidentifiable if their predications are statistically indistinguishable from their limiting cases. When many parameters are unidentifiable, the manifold has a low effective dimensionality because it is narrow in several directions. MBAM aims to approximate a thin manifold by a portion of its boundary by identifying the statistically optimal limiting cases. These approximations reduce the number of parameters in the model while also reducing the computational complexity [24]. For example, approximating a differential variable by an algebraic constraint as is commonly done in singular perturbation. Because MBAM identifies those approximations that are optimal for a particular measurement process, it is a data driven-driven approach that allows us to complement SINDy inferred models with simplified, physics-guided equations.

V. INTEGRATION OF SINDY AND MBAM ALGORITHMS

A flow-chart of the proposed algorithm for the integration of MBAM-based model reduction and SINDy-based model identification is shown in Fig. 1, where particular steps are described in more detail in the sequel.

In the initial step (Step 1, Fig. 1) data-driven input measurements [y(t)] and initial parameter vector (p) are provided.

Please note that SINDy and MBAM algorithms require that state derivatives $[\dot{\boldsymbol{x}}(t)]$ and algebraic variables $[\boldsymbol{z}(t)]$ be calculated. If the state or algebraic variables are not measured directly [part of $\boldsymbol{y}(t)$], then we require at least a local inverse $\begin{bmatrix} \boldsymbol{x}(t) \\ \boldsymbol{z}(t) \end{bmatrix} = \boldsymbol{h}^{-1}[\boldsymbol{y}(t)]$ be available for initial state and algebraic variables (Step 2, Fig. 1) [for example $e'_q(t)$ and $e'_d(t)$ in (A1)], where the time responses from $\boldsymbol{x}(t)$ are later used for calculation $\dot{\boldsymbol{x}}(t)$, by (8). These variables are recalculated in Step 4.

In *Step 3*, we apply the MBAM method to the physics-based dynamics in (1)–(3).

Let there be the fixed, physics-based part of the model [states x_F —for example, three- or four-order SG's dynamic model in Appendices A, B]

$$\dot{\boldsymbol{x}}_F = \boldsymbol{f}_0 \ (\boldsymbol{x}_F, \boldsymbol{z}', \boldsymbol{p}, t) \tag{15}$$

$$\mathbf{0} = \mathbf{g}'(\mathbf{x}_F, \mathbf{z}', \mathbf{p}, t) \tag{16}$$

$$y = h(x_F, z', p, t) \tag{17}$$

where in some cases the set of algebraic constraints (g) (2) may be extended to g' (16) with an augmented vector of algebraic variables (z')—for typical example see (A4). However, the solution of (15)–(17) may turn out to be unfeasible, meaning that the reduced model is unable to satisfy the equality constraints (2) and the available measurements (3) for the full DAEs-based

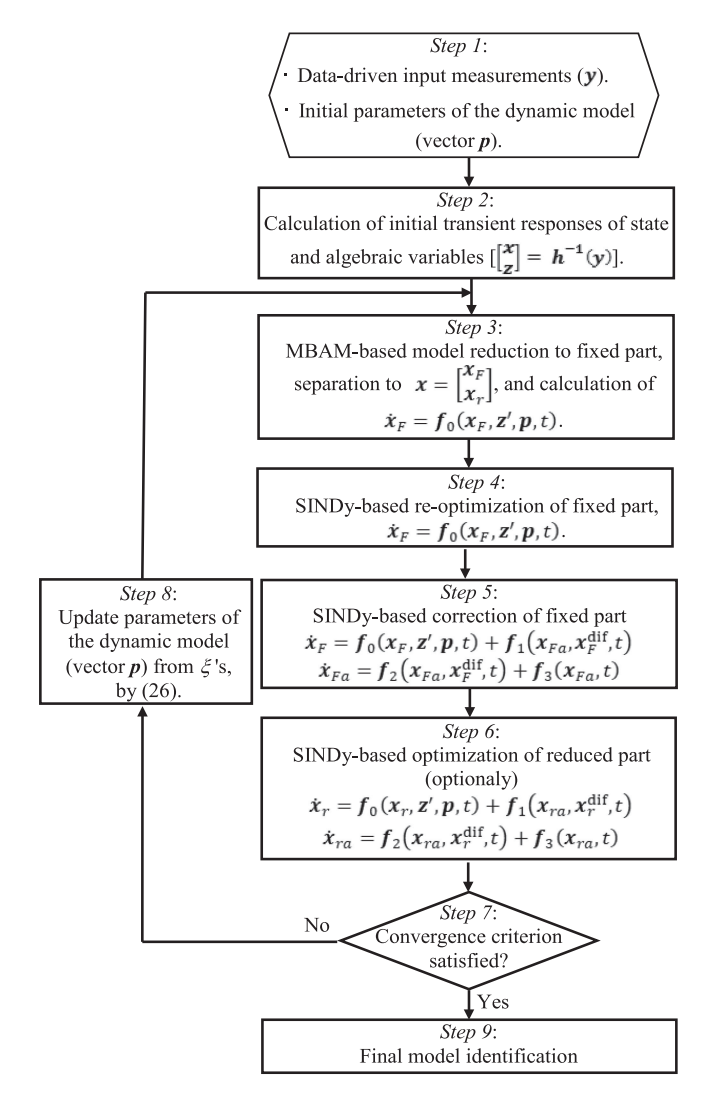


Fig. 1. Integration of MBAM-based model reduction (Section IV) and SINDy-based model identification (Section III-C).

model. This may be improved in *Step 4*, when SINDy will reconsider the MBAM identified fixed part of the model, and in the optional *Step 6* when the MBAM-reduced part of the DAEs-based model is reconsidered.

For single SG we may additionally minimize the discrepancies between measurements (y) and their functions $[h(x_F, z', p, t) \text{ in } (17)]$ in the point of connection to the power system [for example, for active, $P_g(t)$ and reactive, $Q_g(t)$ power generations]. Therefore the transient analysis (15)–(17) is redefined as in $Step\ 4d$ later.

Step 4 (Fig. 1) is performed by the following sub-steps:

Step 4a: Calculation of initial conditions of state (x_0) and algebraic variables (z_0) from available measurements (y) by the extended power flow equations [25, Section 15.1.2].

Step 4b: Numerical calculation of $\dot{x}_F(t)$ by (8). Calculation of non-measured algebraic variables from z'(t) [in analyzed MBAM-based reduced SG test example, the calculation of the algebraic equation for e'_q in (A4)].

Step 4c: SINDy-based model identification $(\Xi_{x,z',y})$ of N_{xF} fixed differential equations, $N_{z'}$ algebraic equations, and N_y

measurements by the optimization model

$$\boldsymbol{\xi}_{n} = \underset{\boldsymbol{\xi}_{n}}{\operatorname{argmin}} \|\boldsymbol{\Theta}(\boldsymbol{X}_{F}, \boldsymbol{Z}', \boldsymbol{Y})_{n} \boldsymbol{\xi}_{n} - \left[\dot{\boldsymbol{X}}_{F} \ \boldsymbol{Z}' \ \boldsymbol{Y}\right]_{n}\|_{2}^{2} + \lambda^{2} \|\boldsymbol{\xi}_{n}\|_{1}; \ n = 1, 2, \cdots, (N_{xF} + N_{zI} + N_{y})$$
(18)

subject to

$$\mathbf{g}'\left(\mathbf{X}_{F}, \mathbf{Z}', \mathbf{p}, t\right) = \mathbf{0} \tag{19}$$

$$\boldsymbol{\xi}_n^{\min} \le \boldsymbol{\xi}_n \le \boldsymbol{\xi}_n^{\max} \tag{20}$$

Step 4d: Minimization of weighted square differences (Dif) between measured time series [y(t)] and ones calculated by fixed part of the identified reduced model (superscript 'c') in Step 4c, $(\Xi_y\Theta_y)$, for $t>t_0$ (the initial condition excluded), is proposed as (to simplify notation, the time dependence of all variables is suppressed)

$$Dif = \underset{\boldsymbol{x}_{y}^{c}, \boldsymbol{z}^{c}}{\operatorname{argmin}} \| \boldsymbol{w} \left(\boldsymbol{y} - \boldsymbol{\Xi}_{\boldsymbol{y}} \boldsymbol{\Theta}_{\boldsymbol{y}} \right) \|_{2}^{2}$$
 (21)

subject to

$$\dot{\boldsymbol{x}}_F^{\mathrm{c}} = \boldsymbol{\Xi}_{\boldsymbol{x}F} \, \boldsymbol{\Theta}_{\boldsymbol{x}F} \tag{22}$$

$$z^{\prime c} = \Xi_{z'} \Theta_{z'} \tag{23}$$

where

w

vector of weighting factors for analyzed measurements;

$$\boldsymbol{\Xi}_{\boldsymbol{x},\boldsymbol{z}',\boldsymbol{y}} = [\, \boldsymbol{\Xi}_{\boldsymbol{x}F} \; \boldsymbol{\Xi}_{\boldsymbol{z}'} \; \boldsymbol{\Xi}_{\boldsymbol{y}}]$$

matrix of calculated parameters for the regression model identification in $Step\ 4c$, and

 $\Theta_{\boldsymbol{x}F},\,\Theta_{\boldsymbol{z}'},\,\Theta_{\boldsymbol{y}}$

vector of functions in a library of K candidate constant, linear, and non-linear functions (with time response values) $\Theta(X_F, Z', Y)$ (Step 4c).

For a practical example of the proposed optimization (21)–(23), please see (21a), (22a-c), and (23a) in Section VI-B.

Notice that in the equality constraints (23) are excluded ones from the measurement set {in analyzed SG test example, the measurements of active, $P_g(t)$ and reactive, $Q_g(t)$ powers are part of equality constraints [g in (2)] and measurement set [h in (3)]}.

Step 4e: Based on the optimized fixed part of the state (22) and algebraic variable time responses (23), calculation of the differences between initial (for full model) state and algebraic variable time responses (from Step 2) and ones calculated by the reduced model, respectively as

$$\boldsymbol{x}_{F}^{\mathrm{dif}}(t) = \boldsymbol{x}_{F}(t) - \boldsymbol{x}_{F}^{\mathrm{c}}(t) \tag{24a}$$

$$\mathbf{z}^{\prime \text{dif}}\left(t\right) = \mathbf{z}^{\prime}\left(t\right) - \mathbf{z}^{\prime \text{c}}\left(t\right) \tag{24b}$$

Step 4f: Parameters of the regression model are functions of the parameter vector (p) as a set of non-linear equations

$$\boldsymbol{\xi}_n = f\left(\boldsymbol{p}\right),\tag{25}$$

 $n=1, 2, \ldots, (N_{xF}+N_{z'}+N_y)$ where the number of non-zero elements in the above equations is larger than the number of elements in vector \boldsymbol{p} .

The optimal parameters are calculated by

$$\mathbf{p} = \underset{\mathbf{p}}{\operatorname{argmin}} \| \boldsymbol{\xi} - f(\mathbf{p}) \|_{2}^{2}$$
 (26)

where the elements of vector $\boldsymbol{\xi}$ are only non-zero elements from $\boldsymbol{\xi}_n$'s (matrix $\boldsymbol{\Xi}$ composed with column-vectors $\boldsymbol{\xi}_n$).

These parameters are used for checking the convergence criterion in *Step 7*, Fig. 1.

Next, we consider the case when the initial DAEs-reduced model f_0 in (15) is not satisfactory and want to use data (via extended SINDy) to improve it (*Step 5*, Fig. 1). Let there be the suited model (states x_F) and the additional data-driven part

$$\dot{\boldsymbol{x}}_F = \boldsymbol{f}_0 \left(\boldsymbol{x}_F, \boldsymbol{z}', \boldsymbol{p}, t \right) + \boldsymbol{f}_1 \left(\boldsymbol{x}_{Fa}, \boldsymbol{x}_F^{\text{dif}}, t \right) \tag{27}$$

where for nonlinearities of various type one function from f_1 is

$$\boldsymbol{f}_{1i}(\boldsymbol{x}_{Fa}, \boldsymbol{x}_F^{\mathrm{dif}}, t)$$

$$= \alpha_{i0} + \sum_{m=1}^{n_F} \beta_{iFm} \boldsymbol{x}_{Fm}^{\text{dif}} + \sum_{m=1}^{n_F} \sum_{n=1}^{n_a} \beta_{iFa,mn} \boldsymbol{x}_{Fan} \boldsymbol{x}_{Fm}^{dir}$$

$$+ \sum_{m=1}^{n_F} \gamma_{iFm} (\boldsymbol{x}_{Fm}^{\text{dif}})^2 + \sum_{n=1}^{n_{Fa}} \gamma_{ian} \boldsymbol{x}_{Fan}^2 + \cdots$$

$$+ \sum_{n=1}^{n_{Fa}} \delta_{ian} \sin(\boldsymbol{x}_{Fan}) + \sum_{n=1}^{n_{Fa}} \epsilon_{ian} \cos(\boldsymbol{x}_{Fan}) + \cdots ;$$

$$i = 1, 2, \dots, n_{Fa}$$
(2

and n_{Fa} is the number of additional state variables (in x_{Fa}) to the fixed part (in x_F).

We find α 's, β 's, γ 's, δ 's, ε 's, ...,by SINDy-based optimization, and x are a new model

$$\begin{bmatrix} \dot{\boldsymbol{x}}_F \\ \dot{\boldsymbol{x}}_{Fa} \end{bmatrix} = \boldsymbol{f} \left(\boldsymbol{x}_F, \boldsymbol{x}_{Fa}, \boldsymbol{x}_F^{\text{dif}}, \boldsymbol{z}', \boldsymbol{p}, t \right)$$
(29)

or

$$\dot{\boldsymbol{x}}_F = \boldsymbol{f}_0 \left(\boldsymbol{x}_F, \boldsymbol{z}', \boldsymbol{p}, t \right) + \boldsymbol{f}_1 \left(\boldsymbol{x}_{Fa}, \boldsymbol{x}_F^{\text{dif}}, t \right)$$
 (27)

$$\dot{\boldsymbol{x}}_{Fa} = \boldsymbol{f}_2 \left(\boldsymbol{x}_{Fa}, \boldsymbol{x}_F^{\text{dif}}, t \right) + \boldsymbol{f}_3 \left(\boldsymbol{x}_{Fa}, t \right)$$
 (30)

which can be MBAM-ed again, possibly repeatedly.

Optionally, Step 6 may be applied to optimize the reduced part

$$\dot{\boldsymbol{x}}_r = \boldsymbol{f}_0 \left(\boldsymbol{x}_r, \boldsymbol{z}', \boldsymbol{p}, t \right) + \boldsymbol{f}_1 \left(\boldsymbol{x}_{ra}, \boldsymbol{x}_r^{\text{dif}}, t \right)$$
(31)

$$\dot{\boldsymbol{x}}_{ra} = \boldsymbol{f}_2 \left(\boldsymbol{x}_{ra}, \boldsymbol{x}_r^{\text{dif}}, t \right) + \boldsymbol{f}_3 \left(\boldsymbol{x}_{ra}, t \right)$$
 (32)

The convergence criterion in *Step 7* is that the difference of parameters (calculated in *Step 4g*) in two subsequent iterations becomes less than the pre-specified threshold.

VI. APPLICATION

We consider transient stability-related DAE-based dynamic model (1)–(3) in a Matlab-derived simulation environment. The proposed algorithm was tested on a real-world test system

(Electric Power Industry of Serbia; a part of the ENTSO-E interconnection) with 441 buses, 655 branches (lines and transformers), 67 SGs (37 of four-order dynamic models and 30 of six-order dynamic models), with automatic voltage regulators and turbine-governor dynamic models. The dynamic model has 797/1284 differential/algebraic variables.

Our Matlab-based environment allows for a variety of state variables (x), algebraic variables (z), and measurements (y) for all SGs to be calculated (by transient analysis tool) and used for simulations and verification of the proposed algorithm:

- state variables [vector x(t) in (1)–(3)]:
- rotor angle, $\delta(t)$ and speed, $\omega(t)$;
- transient voltage in q-, $e'_q(t)$ and d-axis, $e'_d(t)$;
- sub-transient voltage in q-, $e''_q(t)$ and d-axis, $e''_d(t)$,
- algebraic variables [vector z(t) in (1)–(3)]:
- bus voltage magnitude, V(t) and angle, $\theta(t)$;
- exciter's output voltage, $v_f(t)$ and turbine-governor's mechanical power, $P_m(t)$;
- recorded measurements [vector y(t) in (3)]:
- state variables for rotor angle, $\delta(t)$ and speed, $\omega(t)$;
- algebraic variables for bus voltage magnitude, V(t) and angle, $\theta(t)$;
- algebraic variables for exciter's output voltage, $v_f(t)$ and turbine-governor's mechanical power, $P_m(t)$;
- mixed variables for active, $P_g(t)$ and reactive, $Q_g(t)$ power generations.

Notice that the above described full DAE-based dynamic model is used to prepare the measurement sets in buses with connected SGs. The proposed algorithm for SG's model identification is based on measurements in SG's point of connection $\{P_g(t); Q_g(t); V(t); \theta(t)\}$, measurements of exciter's output voltage and turbine-governor's mechanical power, $\{v_f(t); P_m(t)\}$, and DAE-based dynamic model of single SG, described in Appendices A and B. Influence of the full power system dynamic is represented by measurements in point of connection.

The proposed methodology is verified on the SG example in bus 35001 (JHDJERG1—SG 1 in hydropower plant "Djerdap I"), with detailed input data given in Appendix C. Transients are prepared by the three-phase short circuit on the SG's connection point, cleared after 250 ms, for full DAE-based dynamic model.

A. Nonlinear (Trigonometric) Terms in Right-Side of DAEs

This group of tests is performed with the four-order dynamic model of the SG example (see Appendix A). Measurements $P_g(t)$, V(t), and $\theta(t)$ are recorded in the SG's point of connection (obtained by simulations with PSAT-based full dynamic model of the power system [25]). For these tests, the reactive power measurement $Q_g(t)$ is not included directly to (A1), where this assumption will be relaxed later in Section VI-B for the bound-constrained least-squares optimization (11)–(13). Note that measurement $P_g(t)$ may be calculated and included directly into differential equations [as a function of measurements V(t), $\theta(t)$, and state variables $e_q'(t)$, $e_d'(t)$ —see (A2) in Appendix A]. However, in this case, quadratic sine and cosine terms need to be included in the SINDy's model library, with additional terms to be identified—see Appendix B. This means

k	$\dot{\delta}$	ώ	$\dot{e_q'}$	$\dot{e_d'}$	P_g	V	θ
Const.	$-\Omega_b \omega_0 = 2\pi 50.1 = -314.159$	$(P_m + D\omega_0)/2H = 0.281$	$v_f/T'_{d0} = 0.436$	0	0	0	0
δ	0	0	0	0	0	0	0
ω	$\Omega_b = 2\pi 50 = 314.159$	-D/2H = -0.152	0	0	0	0	0
e_q'	0	0	$-x_d/(T'_{d0}x'_d) = -0.516$	0	0	0	0
e_d'	0	0	0	$-x_q/(T'_{q0}x'_q) = -9.250$	0	0	0
P_g	0	-1/2H = -0.080	0	0	1	0	0
V	0	0	0	0	0	1	0
θ	0	0	0	0	0	0	1
$V\cos(\delta-\theta)$	0	0	$(x_d - x_d')/(T_{d0}'x_d') = 0.360$	Ō	0	0	0
$V\sin(\delta-\theta)$	0	0	0	$(x_q - x_q')/(T_{q0}' x_q') = 4.250$	0	0	0

TABLE I EXPECTED MODEL IDENTIFICATION (MATRIX $\Xi_{x,z,y}$) FOR LINEAR AND NONLINEAR (TRIGONOMETRIC) TERMS IN RIGHT-SIDE OF DAES

that first set of tests for verification of software for basic SINDy formulation (Section III-A) is performed with measurement $P_g(t)$ and neglected the equality constraints (A2) and (12). This assumption will be relaxed in Section VI-B. Exciter's output voltage in (A1), is set to be constant, $v_f=1.4998$ pu. For turbine-governor's mechanical power in (A1), we also use a constant value, $P_m=1.6$ pu. Relaxation of these assumptions is straightforward [measurements $v_f(t)$ and $P_m(t)$ simply extend the measurement vector (y)—see Section VI-B].

In this case, there are four derivatives of state variables (vector \dot{x}) and three measurements (vector y) ($\dot{\delta}$, $\dot{\omega}$, \dot{e}'_q , \dot{e}'_d , P_g , V, and θ , respectively) and K=10 elements in a library of candidate nonlinear functions in $\Theta(X,Y,Z)$ (10) {Const.; δ ; ω ; e'_q ; e'_d ; P_g ; V; θ ; $V\cos(\delta-\theta)$, and $V\sin(\delta-\theta)$ }—for details, see Appendix B. Expected model identification [matrix $\Xi_{x,z,y}$ in (10)] for linear and nonlinear (trigonometric) terms in the right-side of the DAEs is shown in Table I.

Based on the analysis in Section III-B, we investigate the following software tools for the specified equality un-constrained (12) and non-bounded (13) identification problem (10):

- 1) SINDy solvers from [13] and [20].
- 2) Lasso software with/without a warm start [26].
- 3) Constrained Lasso, with [27]:
 - a) qp_solver.
 - b) qp_solver with lsqsparse MEX for FORTRAN code from GUROBI.
 - c) using the alternating direction method of multipliers.
- 4) Constrained linear least-squares optimization (Matlab's lsqlin function).
- 5) Regularized Ridge regression [28].

Note that in the analyzed case, $[\dot{\boldsymbol{X}} \boldsymbol{Z} \boldsymbol{Y}]$ is (208×7) -dimensional matrix and $\boldsymbol{\Theta}(\boldsymbol{X}, \boldsymbol{Z}, \boldsymbol{Y})$ is (208×10) -dimensional matrix, where $k = 1, 2, \cdots K = 10$ is the total number of constant, linear, and non-linear (mixed trigonometric) terms in right-side of DAEs, $N_x + N_z + N_y = 7$, and $N_t = 208$.

Results in the form of (10×7) -dimensional matrix $\Xi_{x,z,y}$, where K=10 is the total number of constant, linear and non-linear (mixed trigonometric) terms used in right-side of DAEs and $N_x + N_z + N_y = 7$ is the total number of analyzed state variables (N_x) , algebraic variables (N_z) and measurements (N_y) , obtained by the previously mentioned software tools, are shown in Table II.

We may conclude that used solvers are inefficient for specified SG's equality un-constrained and non-bounded model identification. This condition may be improved by fixing, for example, the parameter Ω_b in the equation for $\dot{\delta}$ (A1), but similar problems remain (see clarification in Section III-B).

Based on the previously derived conclusions, the optimization problem with additional constraints (11)–(13) is specified. The optimization criterion (11) and equality constraints (12) may be transformed into an augmented formulation (14), with lower/upper bounds (13). This problem is adopted for the bound-constrained least-squares optimization [29]

$$\underset{x}{\text{minimize}} \| Ax - b \|_2^2 \tag{33}$$

subject to

$$l \preccurlyeq x \preccurlyeq u \tag{34}$$

where l and u are vectors of lower and upper bounds with the same dimension as vector x, respectively.

Note that this solver is not sparse oriented. However, sparsity [term $\lambda^2 \|\xi_k\|_1$ in (11)] is controlled by the boundary constraints (13)

Results of the SG's equality un-constrained and non-bounded model identification in the form of (10×7) -dimensional matrix $\Xi_{x,z,y}$ are shown in Table III, where all parameters (including Ω_b) are optimized. Comparing with expected values in Table I, these results are much better than those in Table II. The average mean square error (MSE) between measurements and calculated time responses by the identified model is MSE = 0.0132.

The computation time for the SG's model identification is approximately 2.1 s (independent on the operational condition), recorded on the machine with performances: Intel(R) Core(TM) i7-6860HQ CPU @ 2.70 GHz, 64-bit Operating System, 32 GB RAM. This computation time suggests near-real-time feasibility of the proposed model identification.

Influence of noise input data to SG's model identification is shown in Table IV for several characteristic intervals of random errors in input transient series $[\dot{X}\ Z\ Y]_n$ (11), in a library of dynamical elements $\Theta(X,Z,Y)_n$ (11), and in parameter's lower/upper limits $\xi_n^{\min}/\xi_n^{\max}$ (13). Also, in the last column of Table IV are shown the results for missed damping term (D) in the library of candidate dynamics (influenced terms are shown

TABLE II SG'S EQUALITY UN-CONSTRAINED AND NON-BOUNDED MODEL IDENTIFICATION (MATRIX $\mathbf{\Xi}_{x,z,y}$) BY DIFFERENT SOFTWARE TOOLS

SINDy algorithm [13]									
k	$\dot{\delta}$	ώ	$\dot{e'_q}$	$\dot{e_d'}$	P_g	V	θ		
Const.	-265.442	8.511	-25.564	-65.576	0	0	0		
δ	0	0	0	0.674	0	0	0		
ω	265.447	-7.738	23.006	62.011	0	0	0		
e_q'	0	-0.408	1.251	1.931	0	0	0		
e'_d	0	-1.290	4.656	5.426	0	0	0		
P_g	0	0	0	-0.210	1.000	0	0		
V	0	0	0	-0.453	0	1.000	0		
θ	0	0	0	0	0	0	1.000		
$V\cos(\delta-\theta)$	0	0	0	0.186	0	0	0		
$V\sin(\delta-\theta)$	0	0	0	-0.322	0	0	0		
Lasso software [26]									
k	$\dot{\delta}$	ώ	$\dot{e_q'}$	$\dot{e'_d}$	P_g	V	θ		
Const.	0	0	0	0	0	0	0		
δ	0.147	-0.051	0.244	0.501	0	0	0		
ω	266.130	-4.949	2.749	385.622	0	0	0		
e_q'	0.277	-0.187	0	0	0	0	0		
e'_d	-0.241	-0.881	1.363	1.235	0	0	0		
P_g	0	0	0	0	0.971	0	0		
V	0.0551	0	0	0	0	0.971	0		
θ	0	0	0	0.240	0	0	0.971		
$V\cos(\delta-\theta)$	0	0	0	0	0	0	0		
$V\sin(\delta-\theta)$	0	0	0	0	0	0	0		
Constrained I			ab's qp_se e from GU			arse MI	EX for		
k	$\dot{\delta}$	$\dot{\omega}$	$\dot{e_q'}$	$\dot{e'_d}$	P_g	V	θ		
Const.	-314.128	0.211	0.268	1.222	0	0	0		
δ	0	0	0.061	0.916	0	0	0		
ω	314.145	-0.129	0	-0.669	0	0	0		
e_q'	0	0	-0.476	-0.527	0	0	0		
$e_d^{'}$	0	0	0	-3.063	0	0	0		
P_g	0	-0.053	-0.168	0.058	1.000	0	0		
V	0	-0.050	0.203	0.052	0	0.999	0		
θ	0	0	0	0.196	0	0	0.915		
$V\cos(\delta-\theta)$	0	0	0.196	-0.080	0	0	0		
$V\sin(\delta-\theta)$	0.064	-0.055	0.127	-0.098	0	0	0		
	Regul	arized R	idge regre	ssion [28]	•			
k	δ	$\dot{\omega}$	$\dot{e'_q}$.,	P_g	V	θ		
	U	ω	e_q	e_d	* g				
Const.	0	0	e_q	e'_d	1.614	0.982	0.188		
						0.982			
Const. δ	0	0 0	0 0	0	1.614		0.188		
Const. δ	0	0	0	0 0.075	1.614 0	0	0.188		
Const. δ	0 0 0.515	0 0	0 0	0 0.075 0.111	1.614 0 0 0 0	0	0.188 0 0		
Const. δ ω e_q'	0 0 0.515 0	0 0 0	0 0 0 0	0 0.075 0.111 0	1.614 0 0 0	0 0 0	0.188 0 0 0		
Const. δ ω e_q' e_d'	0 0 0.515 0	0 0 0 0	0 0 0 0	0 0.075 0.111 0 0.067	1.614 0 0 0 0	0 0 0 0	0.188 0 0 0		
Const. δ ω e_q' e_d' P_g	0 0 0.515 0 0	0 0 0 0 0	0 0 0 0 0 0 0.076	0 0.075 0.111 0 0.067 -0.080 0	1.614 0 0 0 0 0 0 0.240	0 0 0 0	0.188 0 0 0 0		
Const. δ ω e'_q e'_d P_g V	0 0 0.515 0 0 0	0 0 0 0 0 0	0 0 0 0 0 0 0 0.076	0 0.075 0.111 0 0.067 -0.080	1.614 0 0 0 0 0 0.240	0 0 0 0 0 0	0.188 0 0 0 0 0 0		

in shadowed cells). These results verify the robustness of the proposed approach.

B. Integration of SINDy and MBAM Algorithms

Measurement set [y(t)] is obtained by the six-order state {added sub-transient dynamics by e''_q and e''_d to (A1)—see [24, eq. (15.19)]} and two-order algebraic (A2) SG's dynamic model,

TABLE III SG'S EQUALITY UN-CONSTRAINED AND BOUNDED MODEL IDENTIFICATION (MATRIX $\Xi_{x,z,y}$), Obtained by the CVX Software [29]

k	δ	$\dot{\omega}$	$\dot{e_q'}$	$\dot{e_d'}$	P_g	V	θ
Const.	-314.162	0.281	0.436	0	0	0	0
δ	0	0	0	0	0	0	0
ω	314.156	-0.152	0	0	0	0	0
e_q'	0	0	-0.514	0	0	0	0
e_d'	0	0	0	-9.249	0	0	0
P_g	0	-0.080	0	0	1.000	0	0
V	0	0	0	0	0	1.000	0
θ	0	0	0	0	0	0	1.000
$V\cos(\delta-\theta)$	0	0	0.360	0	0	0	0
$V\sin(\delta-\theta)$	0	0	0	4.250	0	0	0

TABLE IV

SG's Un-Constrained and Bounded Model Identification (Non-Zero Elements in Matrix $\mathbf{\Xi}_{x,z,y}$) Under Noise Input Data and With Missed Damping Term (D) in the Library of Candidate Dynamics, Obtained by the CVX Software [29]

	Basic case (Table III)	±2 %	±5 %	±10 %	Missed damping term (D)
$-\Omega_b\omega_0$	-314.162	-314.162	-312.679	-312.567	-314.162
Ω_b	314.156	314.156	314.156	314.156	314.156
$(P_m + D\omega_0)/2H$	0.281	0.281	0.281	0.281	0.128
− D/2H	-0.152	-0.149	-0.150	-0.140	0
-1/2H	-0.080	-0.079	-0.079	-0.078	-0.080
v_f/T'_{d0}	0.436	0.436	0.436	0.436	0.436
$-x_d/(T'_{d0}x'_d)$	-0.514	-0.513	-0.513	-0.513	-0.514
$(x_d - x_d')/(T_{d0}' x_d')$	0.360	0.359	0.359	0.359	0.360
$-x_q/(T'_{q0}x'_q)$	-9.250	- 9.197	-9.150	-8.806	-9.250
$(x_q - x_q')/(T_{q0}'x_q')$	4.250	4.250	4.250	4.250	4.250
MSE	0.0132	0.0151	0.0193	0.0365	0.0136

TABLE V

SINDy-Based SG's Equality Constrained and Bounded Model Identification for MBAM-Based Reduced Three-Order SG Model From (A3), (A4) (Matrix $\boldsymbol{\Xi}_{x,z',y}$) After Step 4C (Fig. 1), Obtained by the CVX Software [29]

	-							
	δ	$\dot{\omega}$	$\dot{e_d'}$	e_q'	P_g	Q_g	v_f	P_m
Const.	-314.162	0.151	0	0	0	0	0	
δ	0	0	0	0	0	0	0	
ω	314.156	-0.154	0	0	0	0	0	
e_q'	0	0	0	0	0	0	0	
e_d'	0	0	-9.342	0	0	0	0	
P_g	0	0	0	0	0	0	0	
Q_g	0	0	0	0	0	0	0	
v_f	0	0	0	0.297	0	0	1.000	
P_m	0	0.079	0	0	0	0		1.000
$V\sin(\delta-\theta)^*$	0	0	4.207	0	0	0	0	
$V\cos(\delta-\theta)$	0	0	0	0.707	0	0	0	
$Ve_q'\sin(\delta-\theta)$	0	-0.404	0	0	5.043	0	0	İ
$Ve_q'\cos(\delta-\theta)$	0	0	0	0	0	5.145	0	
$Ve_d'\sin(\delta-\theta)$	0	0	0	0	0	3.838	0	
$Ve'_d\cos(\delta-\theta)$	0	0.302	0	0	-3.838	0	0	
$V^2 \sin(\delta - \theta) \cos(\delta - \theta)$	0	0.103	0	0	-1.307	0	0	
$V^2 \sin(\delta - \theta) \sin(\delta - \theta)$	0	0	0	0	0	-3.762	0	
$V^2\cos(\delta-\theta)\cos(\delta-\theta)$	0	0	0	0	0	-5.043	0	

^{*} Notice that in trigonometric terms the measurements of voltage magnitude, V(t) and phase angle, $\theta(t)$ are included

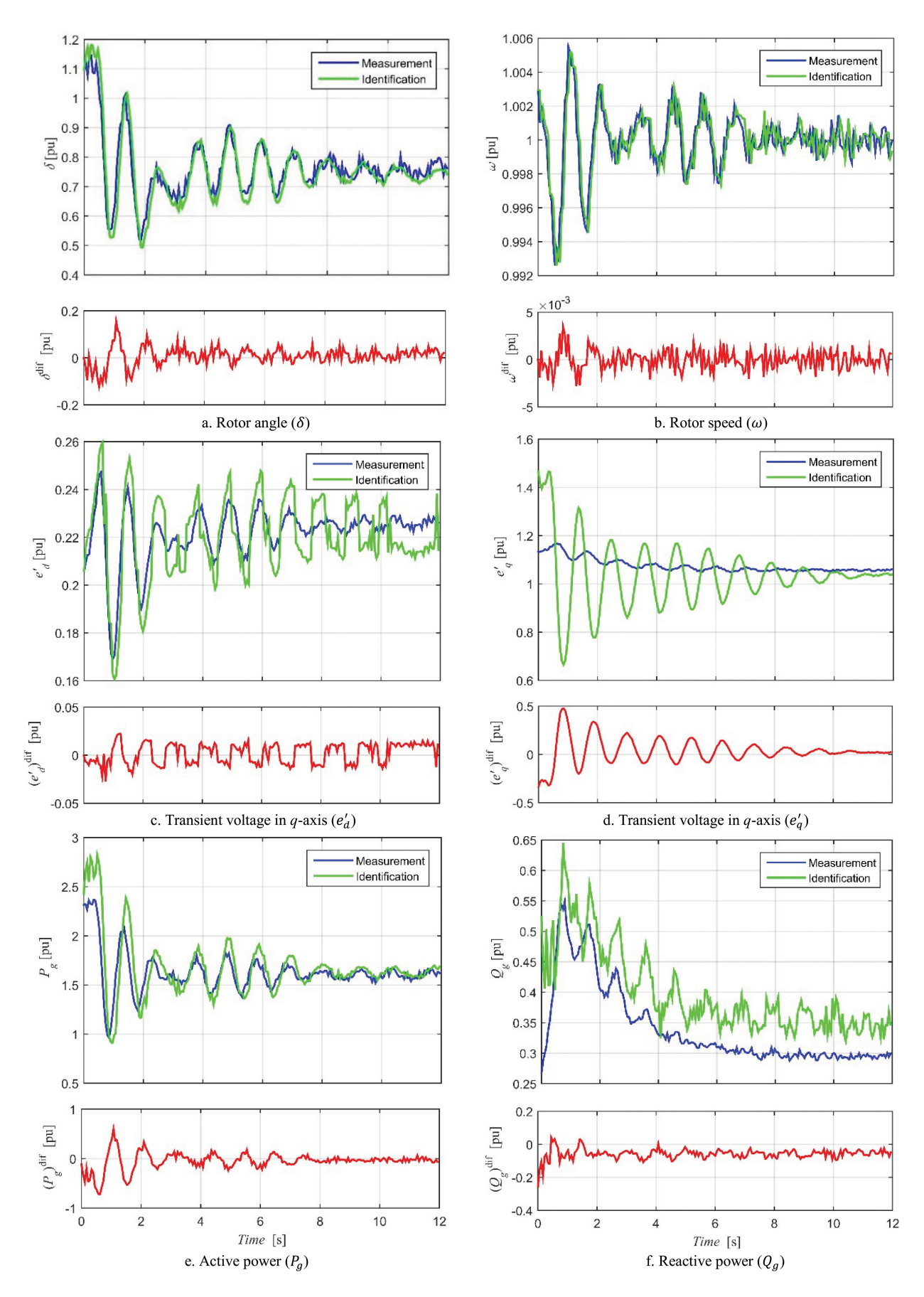


Fig. 2. Measured and identified SG's transient responses of state variables $(\delta, \omega, \text{ and } e'_d)$, state variable reduced to the algebraic variable (e'_q) , and measurements in function both state and algebraic variables [active (P_g) and reactive (Q_g) powers] after fault clearing (top panels) and their differences (bottom panels).

with added a random measurement noise. This DAEs-based SG's dynamic model is reduced in *Step 3* (Fig. 1) by the MBAM algorithm to [for clarification, see (A3) and (A4)]:

- three differential equations $(\delta, \omega, \text{ and } e'_d)$,
- one differential equation transformed to the algebraic equation $(e'_q; T'_{d0} \to \infty)$ [5],
- measurements of exciter output voltage (v_f) and mechanical power from turbine-governor (P_m) , and
- two retained algebraic equations (P_g and Q_g),

or

$$\begin{split} \dot{\boldsymbol{x}}_F &= \left\{ \dot{\delta}; \dot{\omega}; \dot{e}_d' \right\}; \\ \boldsymbol{g}' &= \left\{ e_q'; P_g; Q_g \right\} \\ \boldsymbol{z}' &= \left[e_q' \ V \ \theta \right]^{\mathrm{T}} \\ \boldsymbol{y} &= \left\{ P_g; Q_g; V; \theta; v_f; P_m \right\} \end{split}$$

with seven parameters: Ω_b , 2H, x'_d , x'_q , x_d , x_q , and T'_{d0} .

The proposed integration requires less data (transient responses of reduced three-order SG dynamic model) and input parameters [23], which has conceptual and computational advantages. Differences in transient responses between measurements and calculated values for the reduced-order dynamic model are estimated by a fully data-driven SYNDy model (the results presented later in Table V).

The expected SG's equality constrained and bounded model identification (11)–(13) (*Step 4c*, Fig. 1) with many more nonlinear (trigonometric) terms in the right-side of DAEs for MBAM-reduced model may be simply identified from (A3) and (A4), similarly as in Table I.

SINDy-based SG's model identification after MBAM-based dynamic model reduction (Step 4c, Fig. 1) is represented by a matrix $\mathbf{\Xi}_{x,z,y}$, with K=18 constant, linear, and non-linear (mixed trigonometric) terms in the right-side of DAEs. Input data for SG's model identification is described by the measurement set (with additional noise) $\mathbf{Y}=\{P_g(t);Q_g(t);V(t);\theta(t);v_f(t);P_m(t)\}$ [note that the algebraic variables (z) are part of the measurement vector (y)]. The optimal solution, obtained by the CVX software [29], is shown in Table V. Please note that our procedure identifies the "right-hand" side of DAEs, and not individual original parameters (as with standard system identification procedures—for example, in [4]).

Measurements {described by the measurement set [Y(t)] in (21)} and MBAM- and SINDy-based identified SG transient responses of state variables $(\delta, \omega, \text{and } e'_d)$, algebraic variable (e'_q) , and mixed variables [active (P_g) and reactive (Q_g) powers], after fault clearing, and their differences are shown in Fig. 2. These transients are obtained by minimizing the weighted differences between measured and values calculated by a fixed part of the reduced model (21), subjected to differential (22) and algebraic constraints (23) (Step 4d). In our case, this optimization is described as in (21a), (22a-c), and (23a) (to simplify notation, the time dependence of all variables is suppressed).

Please note a large discrepancy for e_q' in Fig. 2, because the exciter's output voltage $[v_f(t)]$ is very different for two dynamic models [for example, $v_{f0} = v_f$ (t=0) = 3.168 pu for the sixth-order dynamic model, compared with $v_{f0} = 1.4998$ pu for the fourth-order dynamic model (Section VI-A)]. However,

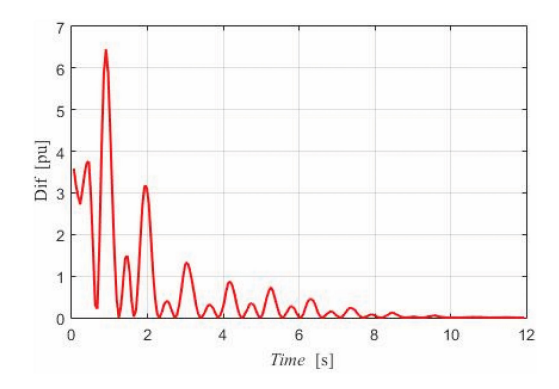


Fig. 3. Optimization criterion $[\mathrm{Dif}(t), t > t_0]$ after minimization of weighted differences between measured values $[P_g(t)]$ and $[P_g(t)]$ and those calculated by fixed part of the reduced model, subject to differential and algebraic equations based constraints.

 $e_q^\prime(t)$ identifies the variable as largely unaffected by tunable model parameters (sloppy) and validates MBAM suggestion to relegate it to algebraic variables. The voltage angle at the point of connection varies considerably during this transient (more than half a radian), meaning that a traditional single-machine infinite-bus-type identification is unlikely to succeed.

$$\min_{\delta,\omega,e'_{d}} \text{ Dif}$$

$$= w_{1} \left(P_{g} - \xi_{12,5} V e'_{q} \sin(\delta - \theta) - \xi_{15,5} V e'_{d} \cos(\delta - \theta) \right)$$

$$- \xi_{16,5} V^{2} \sin(\delta - \theta) \cos(\delta - \theta) \right)^{2}$$

$$+ w_{2} \left(Q_{g} - \xi_{13,6} V e'_{q} \cos(\delta - \theta) - \xi_{14,6} V e'_{d} \sin(\delta - \theta) \right)$$

$$- \xi_{17.6} V^{2} \sin^{2}(\delta - \theta) - \xi_{18.6} V^{2} \cos^{2}(\delta - \theta) \right)^{2}$$
(21a)

subject to differential equation-based constraints (22)

$$\dot{\delta} = \xi_{1,1} + \xi_{3,1}\omega;$$

$$\dot{\omega} = \xi_{1,2} + \xi_{3,2}\omega + \xi_{9,2}P_m + \xi_{12,2}Ve'_q\sin(\delta - \theta)$$

$$+ \xi_{15,2}Ve'_d\cos(\delta - \theta) + \xi_{16,2}V^2\sin(\delta - \theta)\cos(\delta - \theta)$$
(22a)

$$\dot{e}'_d = \xi_{5.4} \, e'_d + \xi_{10.4} V \sin \left(\delta - \theta \right), \tag{22c}$$

and algebraic equation-based constraint (23)

$$e'_{q} = \xi_{83} v_{f} + \xi_{11,3} V \cos(\delta - \theta),$$
 (23a)

where $w_1 = w_2 = 1.0$.

This optimization problem (21)–(23) is solved by Matlabbased 'fmincon' solver (to determine the fitting values for algebraic equations) and 'ode45' integrator (for transient responses of differential equations). The calculated optimization criterion (Dif) is shown in Fig. 3.

Results of MBAM- and SINDy-based identification by only one additional state variable [$x_a = x_{a1}$ in (27), (29), and (30)] for differences of retained state variables (fixed part) and measurements in the function of both state and algebraic variables from Fig. 2 (bottom panels) are shown in Table VI. These differences are completely data-driven (without exact mathematical description) and formal polynomial and trigonometric identification terms are assumed.

TABLE VI

MBAM- AND SINDY BASED IDENTIFICATION (MATRIX $\Xi_{x,z',y}$) OF STATE VARIABLE DIFFERENCES $(\delta,\omega,$ AND $e'_d)$, ALGEBRAIC VARIABLE DIFFERENCES (e'_q) AND MEASUREMENT DIFFERENCES $(P_g$ AND $Q_g)$, AS A FUNCTION OF STATE AND ALGEBRAIC VARIABLES, OBTAINED BY THE SINDY ALGORITHM [13]

k	$\dot{\delta}^{ m dif}$	$\dot{\omega}^{ m dif}$	$(\dot{e_d'})^{ m dif}$	$(e_q')^{ m dif}$	$P_g^{ m dif}$	$Q_g^{ m dif}$
Const.	75.501	-128.478	$-1.406 \cdot 10^3$	$-1.601 \cdot 10^3$	$-3.886 \cdot 10^3$	-460.745
δ	0	0	0	0	4.094	0
ω	-150.980	260.093	$2.867 \cdot 10^3$	$3.210 \cdot 10^3$	$7.749 \cdot 10^3$	929.792
e_q'	0	0	-14.149	-7.788	-28.1950	-7.951
e_d'	0	0	0	0	-1.541	0
δx_{a1}	0	0	0	0	0	0
ωx_{a1}	1.000	0	0	0.592	0	0
$e_q'x_{a1}$	0	0	0	0	0	0
$e'_d x_{a1}$	0	0	0	0	0	0
δ^2	0	0	0	0	-3.421	0
ω^2	75.479	-131.615	$-1.457 \cdot 10^3$	$-1.607 \cdot 10^3$	$-3.860 \cdot 10^3$	-468.273
$(e_{q}')^{2}$	0	0	19.912	15.950	56.381	18.919
$(e'_{d})^{2}$	0	0	0	0	0.633	0
$\frac{(e'_d)^2}{x_{a1}^2}$	0	0	-0.879	0	0	0
$sin(x_{a1})$	0	0	0	-0.563	0	0
$cos(x_{a1})$	0	0	-1.738	0	0	0

TABLE VII SG'S MODEL IDENTIFICATION (NON-ZERO ELEMENTS IN MATRIX $\Xi_{x,z,y}$) FOR REDUCED PART, OBTAINED BY THE CVX SOFTWARE [29]

Coefficient	State/algebraic variables	Expected values	Identified values
$-x_d^{\prime}/(T_{d0}^{\prime\prime}x_d^{\prime\prime})$	$e_q^{\prime\prime}$	-14.655	-14.604
$1/T_{d0}^{"}$	e_q'	11.905	12.021
$(x'_d - x''_d)/(T''_{d0}x''_d)$	$V\cos(\delta-\theta)$	2.750	2.751
$-x_q^{\prime}/(T_{q0}^{\prime\prime}x_q^{\prime\prime})$	$e_d^{\prime\prime}$	-39.290	-39.073
$1/T_{q0}^{\prime\prime}$	e_d'	23.809	23.895
$(x_q^{\prime} - x_q^{\prime\prime})/(T_{q0}^{\prime\prime}x_q^{\prime\prime})$	$V \sin(\delta - \theta)$	15.480	15.490

In the reduced part of the dynamic model (31), there are the following sub-transient state variables in q- and d-axis

$$\boldsymbol{f}_r \Rightarrow \left\{ \begin{array}{l} \dot{e}_q'' = \frac{1}{T_{ro}''} \, \left(-e_q'' + e_q' - \left(x_d' - x_d'' \right) i_d \right) \\ \dot{e}_d'' = \frac{1}{T_{ro}''} \, \left(-e_d'' + e_d' + \left(x_q' - x_q'' \right) i_q \right) \end{array} \right.$$

where
$$i_d=\frac{e_q''-V\cos(\delta-\theta)}{x_d''}$$
 ; $i_q=\frac{V\sin(\delta-\theta)-e_d''}{x_q''}$

Results of the model identification for reduced state variables (Step 6 in Fig. 1) after fault clearing are shown in Table VII. Time responses of state variables (δ , e'_q , and e'_d) and algebraic variables (V and θ) are ones from the optimized fixed part (Step 4, Fig. 1). Measurements and identified SG's transient responses of state variables in reduced part (e''_q and e''_d) after fault clearing are shown in Fig. 4.

VII. CONCLUSION

This paper aims to demonstrate the relevance of the sparse identification of nonlinear dynamics (SINDy) algorithms for data-driven identification of dynamic models used in transient stability of large power systems. We extended the SINDy family of candidate expressions to include products of state and algebraic variables and trigonometric functions of state and algebraic variables, including couplings with exogenous signals

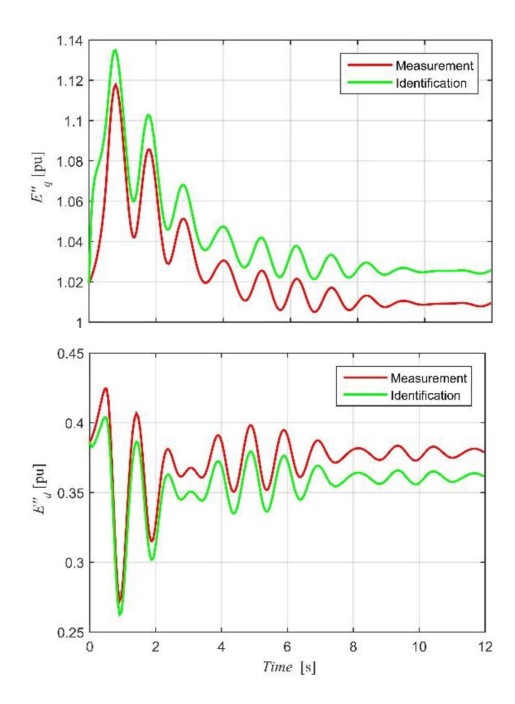


Fig. 4. Measured and identified SG transient responses of state variables in reduced part (e_q'') and e_d'' after fault clearing.

(measurements). The proposed methodology generates models that are sparse by design and aims to identify only a few additional "active" terms in the dynamic response. For that reason, the methodology tends to require fewer data to achieve a good performance than other leading machine learning techniques and seems to be largely immune to overfitting. The proposed model identifies strongly nonlinear systems from local measurement data only, and the model identification is fast enough to discover models in real-time (where the transient responses may be generated continuously by the load/generation increments due to the daily load/generation profiles). The ability to identify effective models from small amounts of data is a very valuable feature in time-critical scenarios, such as in the case of model variations that could render the power system unstable.

APPENDIX

SG's Models and Input Data

A. The Four-Order Model

The four-order differential (motion and electrical) and twoorder algebraic dynamic model (armature resistance r_a is neglected) of SG respectively are [25]:

$$f \Rightarrow \begin{cases} \dot{\delta} = \Omega_{b} \ (\omega - \omega_{0}) \\ \dot{\omega} = \frac{1}{2H} \ (P_{m} - P_{g} - D (\omega - \omega_{0})) \\ \dot{e}'_{q} = \frac{1}{T'_{q0}} \ (-e'_{q} - (x_{d} - x'_{d}) i_{d} + v_{f}) \\ \dot{e}'_{d} = \frac{1}{T'_{q0}} \ (-e'_{d} + (x_{q} - x'_{q}) i_{q}) \end{cases}$$
(A1)

$$g \Rightarrow \begin{cases} P_g = V \sin(\delta - \theta) i_d + V \cos(\delta - \theta) i_q \\ Q_g = V \cos(\delta - \theta) i_d - V \sin(\delta - \theta) i_q \end{cases}$$
(A2)

$$f_{0} \Rightarrow \begin{cases} \dot{\delta} = \Omega_{b} \ (\omega - \omega_{0}) \\ \dot{\omega} = \frac{1}{2H} \left(P_{m} - \frac{Ve'_{q}}{x'_{d}} \sin\left(\delta - \theta\right) + \frac{Ve'_{d}}{x'_{q}} \cos\left(\delta - \theta\right) + V^{2} \left(\frac{1}{x'_{d}} - \frac{1}{x'_{q}} \right) \sin\left(\delta - \theta\right) \cos\left(\delta - \theta\right) - D\left(\omega - \omega_{0}\right) \right) \\ \dot{e}'_{d} = \frac{1}{T'_{q_{0}}} \left(-\frac{x_{q}}{x'_{q}} e'_{d} + \frac{\left(x_{q} - x'_{q}\right)}{x'_{q}} V \sin\left(\delta - \theta\right) \right) \end{cases}$$
(A3)

$$g' \Rightarrow \begin{cases} e'_{q} = \frac{x'_{d}}{x_{d}} v_{f} + \frac{\left(x_{d} - x'_{d}\right)}{x_{d}} V \cos\left(\delta - \theta\right) \\ P_{g} = \frac{V e'_{q}}{x'_{d}} \sin\left(\delta - \theta\right) - \frac{V e'_{d}}{x'_{q}} \cos\left(\delta - \theta\right) - V^{2} \left(\frac{1}{x'_{d}} - \frac{1}{x'_{q}}\right) \sin\left(\delta - \theta\right) \cos\left(\delta - \theta\right) \\ Q_{g} = \frac{V e'_{q}}{x'_{d}} \cos\left(\delta - \theta\right) + \frac{V e'_{d}}{x'_{q}} \sin\left(\delta - \theta\right) - \frac{V^{2}}{x'_{q}} \sin^{2}\left(\delta - \theta\right) - \frac{V^{2}}{x'_{d}} \cos^{2}\left(\delta - \theta\right) \end{cases}$$
(A4)

where

$$i_{d} = \frac{e'_{q} - V\cos(\delta - \theta)}{x'_{d}}$$

$$i_{q} = \frac{V\sin(\delta - \theta) - e'_{d}}{x'_{q}}$$

$$\boldsymbol{x} = \begin{bmatrix} \delta \ \omega \ e'_{q} \ e'_{d} \end{bmatrix}^{\mathrm{T}}$$

$$\boldsymbol{z} = \begin{bmatrix} V \ \theta \end{bmatrix}^{\mathrm{T}}$$

B. The MBAM-Reduced Three-Order Model

The MBAM-reduced three-order SG's differential and three-order algebraic dynamic model [denoted as the fixed part in (16) and (17)] is represented by (A3) and (A4), shown at the top of the page, respectively. where g' is the extended set of algebraic constraints.

C. SG's Input Data

 $S_n=190$ MVA; $V_n=15.75$ kV; f=50 Hz; $\Omega_b=2\pi f=100\pi=314.159;$ $\omega_0=1$ pu; 2H=12.467 MWs/MVA; D=1.9 pu; $T'_{d0}=6.5$ s; $T'_{q0}=0.2$ s; $T''_{d0}=0.084$ s; $T''_{q0}=0.042$ s; $x_d=0.655$ pu; $x_q=0.487$ pu; $x'_d=0.196$ pu; $x'_q=0.263$ pu; $x''_d=0.159$ pu; $x''_q=0.159$ pu.

REFERENCES

- [1] J. J. Sanchez-Gasca, C. J. Bridenbaugh, C. E. J. Bowler, and J. S. Edmonds, "Trajectory sensitivity based identification of synchronous generator and excitation system parameters," *IEEE Trans. Power Syst.*, vol. 3, no. 4, pp. 1814–1822, Nov. 1988.
- [2] S. M. Benchluch and J. H. Chow, "A trajectory sensitivity method for the identification of nonlinear excitation system models," *IEEE Trans. Energy Convers.*, vol. 8, no. 2, pp. 159–164, Jun. 1993.
- [3] I. A. Hiskens, "Nonlinear dynamic model evaluation from disturbance measurement," *IEEE Trans. Power Syst.*, vol. 16, no. 4, pp. 702–710, Nov. 2001.
- [4] M. Burth, G. C. Verghese, and M. Velez-Reyes, "Subset selection for improved parameter estimation in on-line identification of a synchronous generator," *IEEE Trans. Power Syst.*, vol. 14, no. 1, pp. 218–225, Feb. 1999.
- [5] M. K. Transtrum, A. T. Sarić, and A. M. Stanković, "Information geometry approach to verification of dynamic models in power systems," *IEEE Trans. Power Syst.*, vol. 33, no. 1, pp. 440–450, Jan. 2018.
- [6] J. H. Tu, C. W. Rowley, D. M. Luchtenburg, S. L. Brunton, and J. N. Kutz, "On dynamic mode decomposition: Theory and applications," *J. Comput. Dyn.*, vol. 1, no. 2, pp. 391–421, Jun. 2014.
- [7] I.G. Kevrekidis et al., "Equation-free, coarse-grained multiscale computation: Enabling microscopic simulators to perform system-level analysis," Comm. Math. Sci., vol. 1, no. 4, pp. 715–762, 2003.
- [8] E. Kaiser et al., "Cluster-based reduced-order modelling of a mixing layer," J. Fluid Mechanics, vol. 754, pp. 365–414, Sep. 2014.

- [9] H. Arbabi and I. Mezić, "Ergodic theory, dynamic mode decomposition and computation of spectral properties of the Koopman operator," SIAM J. Appl. Dyn. Syst., vol. 16, no. 4, pp. 2096–2126, Nov. 2017.
- [10] B. C. Daniels and I. Nemenman, "Automated adaptive inference of phenomenological dynamical models," *Nat. Commun.*, vol. 6, Aug. 2015, Art. no. 8133.
- [11] J. C. Loiseau and S. L. Brunton, "Constrained sparse Galerkin regression," J. Fluid Mechanics, vol. 838, no. 10, pp. 42–67, Mar. 2018.
- [12] M. Hoffmann, C. Fröhner, and F. Noéd, "Reactive SINDy: Discovering governing reactions from concentration data," *J. Chem. Phys.*, vol. 150, no. 2, pp. 025101–1–025101–12, Jan. 2019.
- [13] S. L. Brunton, J. L. Proctor, and J. N. Kutz, "Discovering governing equations from data by sparse identification of nonlinear dynamical systems," *Proc. Nat. Acad. Sci. USA*, vol. 113, no. 15, pp. 3932–3937, Mar. 2016.
- [14] S. L. Brunton, J. L. Proctor, and J. N. Kutz, "Sparse identification of non-linear dynamics with control (SINDYc)," *IFAC-Papers On-Line*, vol. 49, no. 18, pp. 710–715, Aug. 2016.
- [15] A. M. Stanković, A. A. Sarić, A. T. Sarić, and M. K. Transtrum, "Data-driven symbolic regression for identification of nonlinear dynamics in power systems," in *Proc. IEEE Power Energy Soc. Gen. Meet.*, Aug. 2-6, 2020, pp. 1–5.
- [16] G. Gnecco, V. Kurkova, and M. Sanguineti, "Some comparisons of complexity in dictionary-based and linear computational models," *Neural Netw.*, vol. 24, no. 2, pp. 171–182, Mar. 2011.
- [17] M. Lotfi and M. Vidyasagar, "A fast noniterative algorithm for compressive sensing using binary measurement matrices," *IEEE Trans. Signal Process.*, vol. 66, no. 15, pp. 4079–4089, Aug. 2018.
- [18] S. L. Brunton and J. N. Kutz, Data-Driven Science, and Engineering: Machine Learning, Dynamical Systems, and Control. Cambridge, U.K.: Cambridge Univ. Press, 2019.
- [19] N. M. Mangan, T. Askham, J. L. Brunton, J. N. Kutz, and S. L. Proctor, "Model selection for hybrid dynamical systems via sparse regression," *Proc. Royal Soc. A: Math., Phys. Eng. Sci.*, vol. 475, no. 2223, pp. 1–22, Mar. 2019.
- [20] L. Zhang and H. Schaeffer, "On the convergence of the SINDy algorithm," Multiscale Model. Simul., vol. 17, no. 3, pp. 948–972, Jul. 2019.
- [21] M. K. Transtrum, B. B. Machta, and J. P. Sethna, "Geometry of nonlinear least squares with applications to sloppy models and optimization," *Phys. Rev. E*, vol. 83, no. 3, pp. 036701–1–036701–35, Mar. 2011.
- [22] M. K. Transtrum and P. Qui, "Model reduction by manifold boundaries," Phys. Rev. Lett., vol. 113, no. 9, pp. 098701–1–098701–6, Aug. 2014.
- [23] M. K. Transtrum, A. T. Sarić, and A. M. Stanković, "Measurement-directed reduction of dynamic models in power systems," *IEEE Trans. Power Syst.*, vol. 32, no. 3, pp. 2243–2253, May 2017.
- [24] H. H. Mattingly, M. K. Transtrum, M. C. Abbott, and B. B. Machta, "Maximizing the information learned from finite data selects a simple model," in *Proc. Nat. Acad. Sci.*, vol. 115, no. 8, pp. 1760–1765, Feb. 2018.
- [25] F. Milano, Power System Modelling and Scripting. Berlin, Germany: Springer Science & Business Media, 2010.
- [26] R. Tibshirani, "Regression shrinkage and selection via the Lasso," J. Royal Stat. Soc., Ser. B, vol. 58, no. 1, pp. 267–288, 1996.
- [27] B. R. Gaines, J. Kim, and H. Zhou, "Algorithms for fitting the constrained Lasso," J. Comput. Graph. Statist., vol. 27, no. 4, pp. 861–871, Aug. 2018.
- [28] A. E. Hoerl and R. W. Kennard, "Ridge regression: Biased estimation for nonorthogonal problems," *Technometrics*, vol. 42, no. 1, pp. 80–86, Feb 2000
- [29] M. Grant, S. Boyd, and Y. Ye, "CVX: Matlab software for disciplined convex programming," Version 2.1, Dec. 2018. [Online]. Available: http://cvxr.com/cvx/

Andrija T. Sarić (Member, IEEE) was born in 1962. He received the B.Sc., M.Sc., and Ph.D. degrees in electrical engineering from the University of Belgrade, Belgrade, Serbia, in 1988, 1992, and 1997, respectively. He is currently a Professor of electrical engineering with the Faculty of Technical Sciences, University of Novi Sad, Serbia. His main research interests include power system analysis, optimization, and planning, as well as the application of artificial intelligence methods in these areas. He is an Associate Editor for the IEEE Transactions on Power Systems.

Mark K. Transtrum received the Ph.D. degree in physics from Cornell University, Ithaca, NY, USA, in 2011. He then studied computational biology as a Postdoctoral Fellow from MD Anderson Cancer Center, Houston, TX, USA. Since 2013, he has been with Brigham Young University, Provo, UT, USA. He is currently an Associate Professor of physics and astronomy. His research works include representations of a variety of complex systems including power systems, systems biology, materials science, and neuroscience.

Aleksandar A. Sarić (Student Member, IEEE) received the bachelor's and master's degrees in electrical and computer engineering from the University of Belgrade, Serbia, in 2018 and 2019, respectively. He is currently working toward the Ph.D. degree with the Electrical and Computer Engineering department, Tufts University. His research interests include machine learning, optimization, system control and signal processing.

Aleksandar M. Stanković (Fellow, IEEEE) received the Ph.D. degree in electrical engineering from the Massachusetts Institute of Technology, Cambridge, MA, USA, in 1993. He is currently an A.H. Howell Professor with Tufts University, Medford, MA, USA. He was with Northeastern University, Boston, MA, USA, from 1993 to 2010. He has held visiting positions with the United Technologies Research Center, and at L'Universite de Paris-Sud and Supelec. He is a Co-Editor of book series on power electronics and power systems for Springer. He was an Associate Editor for the IEEE TRANSACTIONS ON POWER SYSTEMS, IEEE TRANSACTIONS ON SMART GRID, and IEEE TRANSACTIONS ON CONTROL SYSTEM TECHNOLOGY for over 20 years.